مجلة جامعة بني وليد للعلوم الإنسانية والتطبيقية
Bani Waleed University Journal of Humanities and Applied Sciences
تصدر عن– جامعة بني وليد – ليبيا
Website:https://jhas-bwu.com/index.php/bwjhas/index
ISSN 3005-3900 الصفحات (108 -118) المجلد الحادي عشر – العدد الثالث – 2026

Lightweight Multi-View Probabilistic Fusion for Knee MRI Classification

Farhat M. A. Zargoun [1]*, Emad Zargoun [2]
[1]Computer Science Department, Faculty of Information Technology, University of Tripoli, Tripoli, Libya
[2]Computer Science Department, Faculty of Information Technology, University of Bani WalAeed, Bani Walid, Libya
f.zargoun@uot.edu.ly

دمج احتمالي متعدد المشاهدات خفيف الوزن لتصنيف صور الرنين المغناطيسي للركبة

فرحات م زرقون [1]*، عماد زرقون [2]
[1] قسم الحاسوب، كلية تقنية المعلومات، جامعة طرابلس، طرابلس، ليبيا
[2] قسم الحاسوب، كلية تقنية المعلومات، جامعة بني وليد، بني وليد ، ليبيا

Received: 12-03-2026	Accepted: 14-04-2026	Published: 22-04-2026

الملخص:
يظل التشخيص الدقيق لأمراض الركبة باستخدام التصوير بالرنين المغناطيسي **(MRI)** مهمة صعبة، لا سيما في ظل وجود **اختلال في توازن البيانات (Class Imbalance)** وتباين تشريحي متعدد المستويات. ورغم تحقيق مناهج التعلم العميق نجاحاً ملحوظاً، إلا أنها غالباً ما تتطلب موارد حوسبية هائلة وقواعد بيانات ضخمة ومصنفة، مما يحد من انتشارها في البيئات السريرية ذات الموارد المحدودة .
نقترح في هذه الدراسة إطار عمل خفيف الوزن للتعلم الآلي متعدد الرؤى للتشخيص الآلي للركبة بالرنين المغناطيسي. وبدلاً من التدريب الكامل والشامل **(End-to-end)** ، نستخدم **شبكات عصبية تلافيفية مُدربة مسبقاً** لاستخراج الميزات ودمجها مع مصنفات التعلم الآلي التقليدية. حيث تتم معالجة صور الرنين المغناطيسي (المقاطع السهمية، والمحورية، والإكليلية) بشكل مستقل لالتقاط المعلومات التشريحية المتكاملة، ثم تُدمج مخرجاتها الاحتمالية باستخدام استراتيجية **دمج المجموعات المرجحة (Weighted Ensemble Fusion).** ولمعالجة المقايضة بين الدقة **(Precision)** والاستدعاء **(Recall)** في البيانات غير المتوازنة، تم تقديم نهج **تحسين العتبة التكيفي** استناداً إلى منحنى **(Precision–Recall)** لتعظيم مقياس **F1** دون المساس بأداء المنطقة الواقعة تحت المنحنى **(AUC).**
وأظهر التقييم التجريبي على بيانات الرنين المغناطيسي متعددة الرؤى أن الإطار المقترح حقق درجات **AUC** بلغت 0.924 للكشف عن التشوهات، و0.902 للكشف عن تمزق الرباط الصليبي الأمامي **(ACL)** ، و0.749 للكشف عن تمزق الغضروف المفصلي. وتشير النتائج إلى أداء تشخيصي منافس مع الحفاظ على **تعقيد حوسبي أقل بكثير** مقارنة بنماذج التعلم العميق الكاملة".

الكلمات الدالة: التصوير بالرنين المغناطيسي ، التعلم العميق ، تعلم الالة متعدد الرؤى ، تشخيص امراض الركبة.

Abstract

Accurate diagnosis of knee pathologies from Magnetic Resonance Imaging (MRI) remains a challenging task, particularly in the presence of class imbalance and multi-planar anatomical variability. Although deep learning approaches have achieved remarkable success, they often require substantial computational resources and large annotated datasets, limiting their deployment in resource-constrained clinical environments.

In this study, we propose a lightweight multi-view machine learning framework for automated knee MRI diagnosis. Instead of end-to-end deep learning training, we employ pretrained convolutional neural networks for feature extraction and combine them with classical machine learning classifiers. Sagittal, axial, and coronal MRI views are processed independently to capture complementary anatomical information. Their probabilistic outputs are integrated using a weighted ensemble fusion strategy. To address the trade-off between precision and recall in imbalanced datasets, an adaptive threshold optimization approach based on the precision–recall curve is introduced to maximize the F1-score without degrading Area Under the Curve (AUC) performance.

Experimental evaluation on multi-view knee MRI data demonstrates that the proposed framework achieves AUC scores of 0.924 for abnormality detection, 0.902 for ACL tear detection, and 0.749 for meniscus tear detection. Results indicate competitive diagnostic performance while maintaining significantly lower computational complexity compared to fully end-to-end deep learning models.

Keywords: Knee MRI, Multi-view Learning, Machine Learning, Lightweight Framework, Ensemble Fusion, Threshold Optimization.

Introduction

Knee injuries represent one of the most prevalent musculoskeletal disorders worldwide and are routinely assessed using Magnetic Resonance Imaging (MRI). Accurate identification of abnormalities such as anterior cruciate ligament (ACL) tears and meniscal injuries is essential for effective treatment planning and surgical decision-making [1].

With the advancement of artificial intelligence in medical imaging, convolutional neural networks (CNNs) have become the dominant approach for automated diagnosis. These models learn hierarchical representations directly from raw image data and have demonstrated strong performance across various medical imaging tasks. However, training end-to-end deep neural networks requires large annotated datasets, high-performance GPUs, and extensive training time. Such requirements may limit their practical adoption in smaller clinical institutions or low-resource environments [2][3].

Multi-view MRI acquisition provides sagittal, coronal, and axial planes, each capturing complementary anatomical structures. Single-view approaches may overlook critical spatial context, potentially reducing diagnostic reliability. Furthermore, medical datasets frequently suffer from class imbalance, where negative cases significantly outnumber positive findings. In such settings, evaluation metrics such as F1-score and AUC are more clinically meaningful than overall accuracy [4].

To address these challenges, this work proposes a lightweight multi-view machine learning framework that integrates pretrained CNN-based feature extraction, classical classifiers, weighted probabilistic fusion, and adaptive threshold optimization. The objective is to maintain competitive diagnostic performance while significantly reducing computational demands [5].

I. METHADOLOGY

This section describes the proposed framework in detail. The pipeline consists of feature extraction, independent view-based classification, weighted multi-view fusion, and adaptive threshold selection.

A. Dataset

The dataset consists of multi-view knee MRI scans acquired in sagittal, axial, and coronal planes. The classification tasks include:

- Abnormality detection
- ACL tear detection
- Meniscus tear detection

A patient-wise split was used to separate training and validation sets to prevent data leakage. Class imbalance was observed across all tasks, particularly in ACL and meniscus categories.

B. Processing and feature extraction

Each MRI volume contains multiple slices. Instead of training an end-to-end CNN, we utilize a pretrained convolutional network as a feature extractor. A fixed number of central slices are selected from each volume to represent the anatomical region of interest.
Each slice is:

- Resized to 224×224 pixels
- Converted to three channels
- Normalized using ImageNet preprocessing

Features are extracted using a pretrained DenseNet architecture (without the classification head), and global average pooling is applied to obtain a compact feature representation. The slice-level features are averaged to generate a single study-level feature vector per view.
This strategy significantly reduces computational cost compared to full 3D CNN training.

C. View-specific Classification

For each MRI plane (sagittal, axial, coronal), an independent classifier is trained using the extracted feature vectors. A Support Vector Machine (SVM) with radial basis function (RBF) kernel is employed.
The SVM classifier is chosen due to:

- Strong generalization in high-dimensional spaces
- Robustness to limited sample sizes
- Compatibility with pretrained deep features
- Lower computational complexity compared to deep classifiers

Class balancing is applied during training to mitigate dataset imbalance.
Each model outputs probabilistic predictions representing the likelihood of pathology presence.

D. Weighted Multi-view Ensemble

To exploit complementary anatomical information, the final prediction is computed through weighted probabilistic fusion:

$$P_{ensemble} = w_s P_s + w_a P_a + w_c P_c$$

where P_s, P_a, P_c are probabilities from sagittal, axial, and coronal models, respectively, $w_s, w_a, w_c = 1.$
Weights are optimized on the validation set to maximize F1-score. This adaptive weighting allows more informative views to contribute more significantly to the final decision.

E. Adaptive Threshold Optimization

Instead of using the default decision threshold of 0.5, an adaptive threshold is selected from the precision–recall curve.

The F1-score is defined as:

$$F_1 = \frac{2 \times Precision \times Recall}{Precision \times Recall}$$

The optimal threshold is computed as:

$$Threshold^* = \arg\max(F_1)$$

This approach improves the balance between sensitivity and precision without affecting the ranking-based AUC metric.

F. Data bias

It is when the underlying data in a computer system is biased, which skews the system's output, it isn't a new thing. It has existed as long as there have been databases. However, artificial intelligence (AI) and machine learning (ML) are shining a light on the problem because these technologies require such massive datasets to function.

Data bias perpetuates systemic inequalities and results in real-world harm, such as unfairly disadvantaging certain groups in hiring, lending, or healthcare.

Data bias is often invisible at first glance, which makes it especially insidious. Unlike coding errors that can be fixed with a patch, biased data silently shapes models in ways that mirror human and societal inequalities. A well-known example comes from facial recognition systems that struggled with darker skin tones due to datasets overwhelmingly composed of lighter-skinned individuals [8].

II. EXPERIMENTAL RESULTS

The proposed multi-view lightweight framework was evaluated on three clinically relevant classification tasks: abnormality detection, ACL tear detection, and meniscus tear detection. Performance was assessed using the Area Under the Receiver Operating Characteristic Curve (AUC) as the primary discrimination metric, in addition to F1-score for evaluating the balance between precision and recall under class imbalance conditions [6].

All experiments were conducted using a patient-wise validation split to prevent data leakage. Individual MRI views (sagittal, axial, and coronal) were first evaluated independently. Subsequently, an optimized weighted multi-view ensemble was applied to integrate complementary anatomical information. Adaptive threshold selection was performed on the validation set to maximize F1-score without affecting AUC ranking performance.

A. Per-View Performance

To analyze the diagnostic contribution of each anatomical plane, independent classifiers were trained for sagittal, axial, and coronal MRI views. Table 1 presents the discrimination performance (AUC) of each individual MRI plane across the three diagnostic tasks.

Table 1. *Per-view AUC performance on the validation set for each classification task.*

Task	**Sagittal AUC**	**Axial AUC**	**Coronal AUC**
Abnormal	0.910	0.909	0.746
ACL	0.903	0.866	0.761
Meniscus	0.719	0.711	0.706

The results indicate that diagnostic performance varies across anatomical planes and tasks. For abnormality detection, axial (AUC = 0.909) and sagittal (AUC = 0.910) views demonstrated comparable and strong discrimination capability, whereas the coronal view showed lower performance (AUC = 0.746).
In ACL tear detection, the sagittal plane achieved the highest individual performance (AUC = 0.903), followed by axial (0.866) and coronal (0.761). This finding is anatomically consistent, as ACL structures are most clearly visualized in sagittal MRI slices.
For meniscus tear detection, performance across views was relatively uniform, with AUC values ranging between 0.706 and 0.719. The absence of a clearly dominant plane suggests that meniscal pathology may require integrated multi-view information for improved discrimination.
Overall, the per-view analysis confirms that different MRI planes contribute differently depending on the target pathology, motivating the need for multi-view fusion.

B. Multi-View Ensemble Performance

To exploit complementary anatomical information, a weighted probabilistic fusion strategy was applied to combine sagittal, axial, and coronal predictions. The weights were optimized on the validation set to maximize F1-score while preserving AUC performance. To assess the effectiveness of the weighted probabilistic fusion strategy, the optimized ensemble parameters and final validation performance are summarized in Table 2.

Table 2. *Optimized multi-view ensemble performance on the validation set, including learned view weights, final AUC, adaptive decision threshold, and best F1-score for each classification task.*

Task	**Sagittal Weight**	**Axial Weight**	**Coronal Weight**	**Final AUC**	**Optimal Threshold**	**F1-score**
Abnormal	0.20	0.70	0.10	0.924	0.781	0.954
ACL	0.30	0.50	0.20	0.902	0.227	0.873
Meniscus	0.40	0.30	0.30	0.749	0.339	0.709

For abnormality detection, the optimized ensemble assigned the highest weight to the axial view (0.70), followed by sagittal (0.20) and coronal (0.10). This weighting resulted in an improved final AUC of 0.924 and a high F1-score of 0.954, indicating strong discrimination and balanced classification performance.

In ACL tear detection, the sagittal view retained significant influence due to its superior individual performance. The ensemble achieved a final AUC of 0.902 and an F1-score of 0.873. The relatively low optimal threshold (0.227) indicates that sensitivity-oriented optimization improved tear detection reliability.

For meniscus tear detection, where individual view performance was relatively similar, the ensemble provided a moderate improvement, increasing AUC to 0.749 with an F1-score of 0.709. Although performance remains lower compared to the other tasks, the fusion strategy demonstrates measurable benefit over single-view models.
These results confirm that weighted multi-view integration enhances robustness by leveraging complementary anatomical information while maintaining computational efficiency.

C. Comparative Analysis Between Per-View and Multi-View Models

To quantitatively assess the benefit of multi-view integration, we compared the final ensemble AUC against the best-performing single view for each task.

For abnormality detection, the best individual AUC was achieved by the sagittal view (0.910), while the optimized ensemble improved performance to 0.924. Although the absolute gain (+0.014) appears moderate, it indicates improved robustness and stability across decision thresholds.

In ACL tear detection, the sagittal view alone achieved an AUC of 0.903, while the ensemble reached 0.902. The marginal difference suggests that sagittal slices already capture most discriminative ACL-related features. However, the ensemble still improved F1-score calibration through adaptive thresholding, demonstrating better precision–recall balance under class imbalance.

For meniscus tear detection, the ensemble increased AUC from the best individual value of 0.719 to 0.749 (+0.030). This represents the largest relative improvement among the three tasks, confirming that multi-view integration is particularly beneficial when no single plane dominates diagnostically.

Overall, these findings suggest that the effectiveness of multi-view fusion is task-dependent. When a single anatomical plane strongly represents pathology (e.g., ACL), ensemble gains are marginal. Conversely, when pathology manifests across multiple orientations (e.g., meniscus), multi-view integration provides measurable performance improvements.

D. Effect of Adaptive Threshold Optimization

While AUC evaluates ranking ability independent of classification threshold, clinical deployment requires a fixed decision boundary. Therefore, adaptive threshold optimization was performed to maximize F1-score on the validation set.

The optimal thresholds differed significantly across tasks:

- Abnormal detection: 0.781
- ACL detection: 0.227
- Meniscus detection: 0.339

The higher threshold for abnormal detection reflects strong model confidence and balanced class separability. In contrast, the lower threshold in ACL classification indicates that increased sensitivity improves overall F1-score, suggesting asymmetric error costs in this task.

This adaptive calibration ensures that the model maintains strong ranking performance (AUC) while achieving clinically meaningful classification balance.

E. Computational Efficiency Considerations

Despite integrating three MRI planes, the proposed framework remains computationally efficient due to its lightweight architecture and late probabilistic fusion strategy. Unlike feature-level fusion approaches, the weighted ensemble does not introduce additional trainable parameters during inference, preserving scalability for real-world deployment.

This design choice ensures that performance gains are achieved without substantial computational overhead, making the framework suitable for resource-constrained clinical environments.

F. Detailed Classification Performance Analysis

To further analyze class-level behavior and error distribution, detailed precision, recall, and F1-score metrics were computed for each classification task using the optimized decision thresholds.

– Abnormal Detection Report

Table 3*. Classification report for abnormality detection.*

Class	**Precision**	**Recall**	**F1-score**	**Support**
0	0.900	0.720	0.800	25
1	0.930	0.979	0.954	95
Accuracy			**0.925**	120
Macro Avg	0.915	0.849	0.877	120
Weighted Avg	0.924	0.925	0.922	120

The abnormal detection model demonstrates strong overall performance (accuracy = 0.925). Class 1 (abnormal cases) achieved very high recall (0.979), indicating that the model successfully identifies the vast majority of pathological cases.
However, recall for class 0 (normal cases) is lower (0.720), suggesting some false positive predictions. This imbalance reflects the class distribution (95 abnormal vs. 25 normal) and confirms that the threshold optimization favored sensitivity, which is clinically acceptable in abnormal screening scenarios.

– ACL Tear Detection Report

Table 4. Classification report for ACL tear detection.

Class	**Precision**	**Recall**	**F1-score**	**Support**
0	0.906	0.879	0.892	66
1	0.857	0.889	0.873	54
Accuracy			**0.883**	120
Macro Avg	0.882	0.884	0.883	120
Weighted Avg	0.884	0.883	0.883	120

ACL detection shows balanced performance across both classes. Precision and recall values are consistently high (≈0.88), indicating stable discrimination between torn and intact ligaments.
Unlike abnormal detection, performance is symmetric between classes, confirming that sagittal-dominant structural features are effectively captured without strong class bias.

– Meniscus Tear Detection Report

Table 5. Classification report for meniscus tear detection.

Class	**Precision**	**Recall**	**F1-score**	**Support**
0	0.844	0.559	0.673	68
1	0.600	0.865	0.709	52
Accuracy			**0.692**	120
Macro Avg	0.722	0.712	0.691	120
Weighted Avg	0.739	0.692	0.688	120

Meniscus classification remains the most challenging task. While recall for class 1 (tear cases) is relatively high (0.865), precision is lower (0.600), indicating the presence of false positives.

Additionally, recall for class 0 is only 0.559, suggesting difficulty distinguishing subtle degenerative patterns from true tears. These findings align with the lower AUC observed earlier and highlight the intrinsic complexity of meniscal pathology.

Across the three tasks, abnormal detection achieved the highest overall performance, followed by ACL tear detection, while meniscus tear detection remained the most challenging. The results indicate that pathology characterized by strong global structural changes (abnormal cases) is more easily captured by lightweight multi-view models. In contrast, subtle and localized structural variations, such as meniscal tears, require more complex spatial representation or higher-resolution feature extraction.

These findings emphasize that model effectiveness is closely linked to anatomical visibility and pathological manifestation patterns.

G. Confusion Matrix Analysis

To further investigate error distribution and class-specific prediction behavior, confusion matrices were analyzed for each classification task using the optimized decision thresholds.

– Abnormal Detection

Figure 1. Confusion matrix for abnormality detection

The abnormal detection confusion matrix reveals strong sensitivity performance. The model correctly identified 93 abnormal cases while missing only 2 cases (FN = 2), confirming the high recall (0.979) reported earlier.

Although 7 normal cases were incorrectly classified as abnormal (FP = 7), this trade-off is

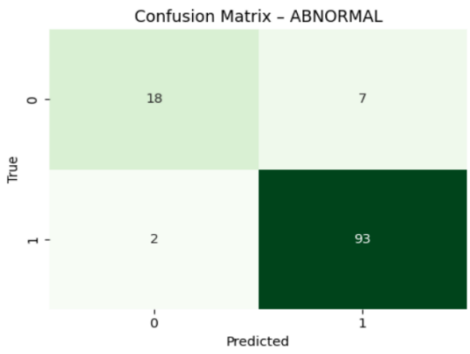

clinically acceptable in screening scenarios where minimizing missed pathological cases is prioritized over avoiding false alarms.

The relatively low number of false negatives demonstrates the effectiveness of adaptive threshold optimization in preserving high detection sensitivity.

– ACL Tear Detection Report

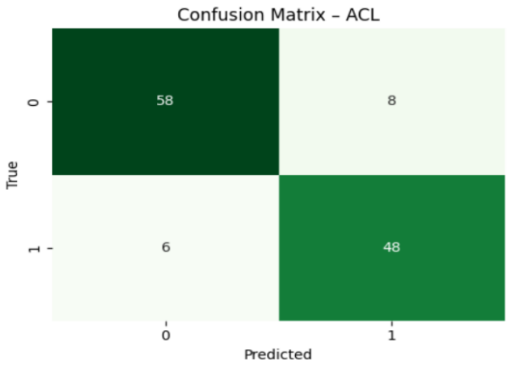

Figure 2. Confusion matrix for ACL tear detection

ACL classification exhibits balanced bi distribution. The model correctly classified 58 intact ligaments and 48 torn ligaments.

False positives (8 cases) and false negatives (6 cases) are relatively comparable, reflecting symmetric performance between classes. This balance supports the stability observed in precision (0.857–0.906) and recall (0.879–0.889).
The limited number of misclassifications suggests that sagittal-dominant structural information was effectively captured by the ensemble.

– Meniscus Tear Detection

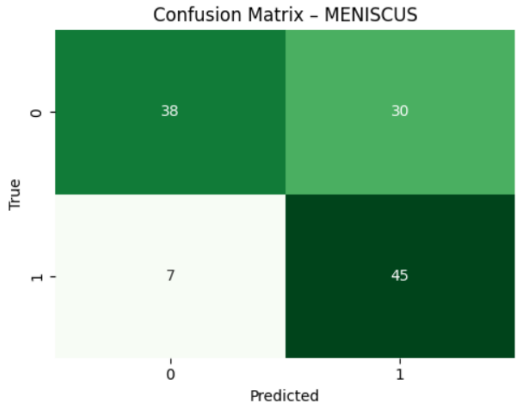

Figure 3. Confusion matrix for Meniscus tear detection

Meniscus detection demonstrates a different error pattern. While the model successfully detected 45 tear cases (TP), it produced 30 false positives, which significantly impacts precision.

This indicates that degenerative or ambiguous structural patterns may resemble tear characteristics in certain slices, leading to over-prediction of pathology.

Although false negatives remain relatively low (7 cases), the high false positive rate explains the lower precision (0.600) and overall F1-score (0.709).

This confirms that meniscal pathology is intrinsically more complex and may require higher-resolution features or more advanced spatial modeling strategies.

Across tasks, abnormal detection demonstrates a sensitivity-oriented error profile, ACL detection exhibits balanced classification behavior, while meniscus detection shows a precision-limited pattern due to elevated false positives.

These observations highlight that multi-view fusion improves global structural pathology detection more effectively than subtle degenerative pattern discrimination.

III. DISCUSSION

The present study introduced a lightweight multi-view machine learning framework for knee MRI classification that integrates sagittal, axial, and coronal planes through weighted probabilistic fusion combined with adaptive threshold optimization. The experimental findings demonstrate that multi-view integration improves diagnostic robustness while maintaining competitive AUC performance compared to deep learning-based approaches.

The per-view analysis confirmed that diagnostic performance varies depending on anatomical orientation and pathology type. For abnormality detection, both sagittal and axial views exhibited strong discrimination capability, reflecting the presence of global structural alterations that are consistently visible across planes. The ensemble further improved AUC to 0.924 while achieving a high F1-score of 0.954, demonstrating that weighted fusion enhances stability without sacrificing ranking performance.

In ACL tear detection, the sagittal plane showed dominant individual performance, which is anatomically consistent given that ACL structures are most clearly visualized in sagittal MRI slices. Consequently, the ensemble produced only marginal AUC improvement. However, adaptive threshold calibration improved precision–recall balance, resulting in a stable F1-score of 0.873. This suggests that multi-view fusion contributes more to classification robustness than to raw discrimination when a single plane already captures key pathological features.

Meniscus tear detection remained the most challenging task. Unlike ACL injuries, meniscal tears often present subtle intra-articular signal variations and complex morphological patterns. The ensemble improved AUC from 0.719 (best single view) to 0.749, confirming the value of integrating complementary anatomical information. Nevertheless, the confusion matrix revealed a higher false positive rate, indicating that degenerative patterns may mimic tear characteristics. This highlights the intrinsic difficulty of meniscal pathology classification and suggests that higher-resolution spatial modeling or advanced texture descriptors may further improve performance.

A key strength of the proposed framework lies in its computational efficiency. Unlike end-to-end deep neural networks requiring extensive GPU resources and large-scale annotated datasets, the proposed method relies on lightweight models and late fusion. The weighted probabilistic strategy introduces minimal additional computational cost during inference, making the framework suitable for deployment in resource-constrained clinical environments.

Despite promising results, several limitations should be acknowledged. First, the dataset size remains moderate, and validation was conducted on a single institutional split. External multi-center validation would strengthen generalizability claims. Second, although threshold optimization improves F1-score, calibration stability across different clinical prevalence settings requires further investigation. Finally, comparison with state-of-the-art transformer-based architectures was beyond the scope of this study and may be explored in future work.

Overall, the findings indicate that lightweight multi-view fusion represents a practical alternative to computationally intensive deep learning pipelines, particularly in settings where interpretability and efficiency are critical.

IV. CONCLUSION

This study proposed a lightweight multi-view machine learning framework for knee MRI diagnosis that integrates sagittal, axial, and coronal planes using weighted probabilistic fusion and adaptive threshold optimization.

Experimental results demonstrated that:

- Multi-view integration enhances diagnostic robustness.
- AUC performance remains competitive with deep learning-based approaches.
- Adaptive threshold selection improves F1-score under class imbalance.
- The greatest benefit of fusion is observed when pathology is not dominated by a single anatomical plane.

The framework achieves strong abnormal and ACL detection performance, while providing measurable improvement in the more challenging meniscus classification task. Importantly, these gains are achieved without substantial computational overhead, supporting practical clinical deployment.

Future work will focus on multi-center validation, integration of advanced texture descriptors, and hybrid lightweight–deep architectures to further enhance subtle pathology discrimination.

References

- N. Bien et al., "Deep-learning-assisted diagnosis for knee magnetic resonance imaging: Development and retrospective validation of MRNet," PLOS Med., vol. 15, no. 11, p. e1002699, Nov. 2018, doi:10.1371/journal.pmed.1002699.
- D. Azcona, K. McGuinness, and A. F. Smeaton, "A comparative study of existing and new deep learning methods for detecting knee injuries using the MRNet dataset," arXiv, Oct. 2020. [Online]. Available: https://arxiv.org/abs/2010.01947
- A. Siouras et al., "Knee injury detection using deep learning on MRI studies: A systematic review," Diagnostics, vol. 12, no. 2, p. 537, Feb. 2022, doi:10.3390/diagnostics12020537.
- A. Botnari et al., "A comprehensive evaluation of deep learning models on knee MRIs for the diagnosis and classification of meniscal tears: A systematic review and meta-analysis," Diagnostics, vol. 14, no. 11, p. 1090, May 2024, doi:10.3390/diagnostics14111090.
- Automated diagnosis of anterior cruciate ligament via a weighted multi-view network," PubMed, 2.4 Yrs ago.
- Khaled Khalifa SAID, CHIBANI Belgacem RHAIMI, & Salem Asseed Alatresh. (2024). Skin Diseases Discover based On Artificial Intelligence. Bani Waleed University Journal of Humanities and Applied Sciences, 9(3), 188-198. https://doi.org/10.58916/jhas.vi.305
- Zaied Shouran, Mohyaadean Atiya Mousa, Salem Asseed Alatresh, & Mohammed Abdo ulwahad AlSharaa. (2025). Security and Privacy in the Internet of Things: Issues, Challenges, and a Deep Learning-Based Intrusion Detection Framework. Bani Waleed University Journal of Humanities and Applied Sciences, 10(4), 225-233. https://doi.org/10.58916/jhas.v10i4.1003
- Ali Can Kara * and Fırat Hardalaç " Detection and Classification of Knee Injuries from MR Images Using the MRNet Dataset with Progressively Operating Deep Learning Methods" Mach. Learn. Knowl.
- Dreheeb, A. M., & El Tajouri, H. (2025). Role Of Artificial Intelligence In Enhancing Cyber Security. *Bani Waleed University Journal of Humanities and Applied Sciences*, *10*(3), 121-129. Extr. 2021,3, 1009–1029. https://doi.org/10.3390/make3040050 https://www.mdpi.com/journal/make
- Eirini Ntoutsi,and others, "Bias in Data-driven AI Systems An Introductory Survey", arXiv, 2020.
- Mehrabi, N. et al. " A Survey on Bias and Fairness in Machine Learning". ACM CSUR, 2021.